JOURNAL OF BACTERIOLOGY, Sept. 2002, p. 5027–5035 Vol. 184, No. 18
0021-9193/02/$04.00+0 DOI: 10.1128/JB.184.18.5027–5035.2002

A Novel Histidine-Rich CPx-ATPase from the Filamentous Cyanobacterium *Oscillatoria brevis* Related to Multiple-Heavy-Metal Cotolerance

Liu Tong, Susumu Nakashima, Mineo Shibasaka, Maki Katsuhara, and Kunihiro Kasamo*

Research Institute for Bioresources, Okayama University, Kurashiki, Okayama 710-0046, Japan

Received 22 April 2002/Accepted 21 June 2002

A novel gene related to heavy-metal transport was cloned and identified from the filamentous cyanobacterium *Oscillatoria brevis*. Sequence analysis of the gene (the Bxa1 gene) showed that its product possessed high homology with heavy-metal transport CPx-ATPases. The CPC motif, which is proposed to form putative cation transduction channel, was found in the sixth transmembrane helix. However, instead of the CXXC motif that is present in the N termini of most metal transport CPx-ATPases, Bxa1 contains a unique Cys-Cys (CC) sequence element and histidine-rich motifs as a putative metal binding site. Northern blotting and real-time quantitative reverse transcription-PCR showed that expression of Bxa1 mRNA was induced in vivo by both monovalent (Cu^+ and Ag^+) and divalent (Zn^{2+} and Cd^{2+}) heavy-metal ions at similar levels. Experiments on heavy-metal tolerance in *Escherichia coli* with recombinant Bxa1 demonstrated that Bxa1 conferred resistance to both monovalent and divalent heavy metals. This is the first report of a CPx-ATPase responsive to both monovalent and divalent heavy metals.

Organisms usually utilize emergency mechanisms such as reduced uptake, facilitated efflux, sequestration, and modification to achieve resistance to the toxicity of heavy metals (5, 22, 27, 37). Heavy-metal transport P-type ATPases (or CPx-ATPases) are thought to act as a potential key heavy-metal transporter involved not only in metal ion homeostasis but also in the overall strategy for heavy-metal tolerance (3, 37).

CPx-ATPases are a new subgroup of P-type ATPases and possess all the common characteristics of P-type ATPases (25, 37). One significant difference, however, is the presence of a conserved intramembranous cysteine-proline-cysteine/histidine/serine (CPx) motif. P-type ATPases with this unique characteristic are therefore termed CPx-ATPases. Another unique feature of CPx-ATPases is the N-terminal metal binding domain. In most cases, the heavy-metal binding domain consists of one or several cysteine-rich (CXXC) motifs. In certain cases, the cysteine-rich N terminus is replaced by a short sequence containing histidine.

There is currently great interest in the N-terminal-cysteine-rich CPx-ATPases (1, 6, 9, 17, 31); however, little interest has been paid to the N-terminal-histidine-rich CPx-ATPases. Recently, genomic DNA programs have revealed that the N-terminal-histidine-rich CPx-ATPases are also distributed widely among organisms (8, 10, 11, 37, 38), especially plants, although the true roles of these CPx-ATPases are not yet known.

Although the detailed characterization of CPx-ATPases is still awaited, the main physiological function of these enzymes is thought to be the transport of heavy-metal ions across biological membranes to maintain the intracellular homeostasis of essential or nonessential heavy metals and deliver specific metal ions to target enzymes. CPx-ATPases have been found to have high specificity for the heavy-metal ions they transport. It has been demonstrated that the type of transport substrate is restricted by heavy-metal ion valence (1, 24, 29, 35). CPx-ATPases can be divided into two classes: those that transport monovalent heavy metals such as Cu^+ and Ag^+ and those that transport divalent heavy metals such as Zn^{2+} and Cd^{2+}. No report so far has shown that a CPx-ATPase responds to both divalent and monovalent heavy-metal ions. The mechanisms of metal ion specificity remain to be established.

The filamentous cyanobacterium *Oscillatoria brevis* has multiple-heavy-metal cotolerance, especially to Cd, Zn, Cu, and Ag ions (data not shown). *O. brevis* belongs to a family of musty-odor-producing cyanobacteria (18). These cyanobacteria affect the quality of drinking water (19). Copper sulfate is commonly used in water purification systems as a cyanobacterial algicide, but the basic mechanism of heavy-metal homeostasis and resistance in cyanobacteria is still unknown.

In this study, we have identified and characterized a novel gene encoding a heavy-metal transport CPx-ATPase from *O. brevis* named Bxa1 (*O. brevis* multiplex heavy-metal transport ATPase 1). Sequence analysis shows that Bxa1 has high homology with other heavy-metal transport CPx-ATPases, including a unique CPC motif and HP locus. However, in the N-terminal heavy-metal binding region, it possesses a Cys-Cys (CC) sequence element and histidine-rich motif instead of the CXXC segment or low-density histidine-containing motif. The expression of Bxa1 is induced by both monovalent (e.g., Cu^+ and Ag^+) and divalent (e.g., Zn^{2+} and Cd^{2+}) cations in vivo. Heavy-metal tolerance experiments on *Escherichia coli* with recombinant Bxa1 demonstrated that Bxa1 expression conferred tolerance to both monovalent and divalent heavy met-

* Corresponding author. Mailing address: Research Institute for Bioresources, Okayama University, Kurashiki, Okayama 710-0046, Japan. Phone: 81-86-434-1221. Fax: 81-86-434-1221. E-mail: kasamo@rib.okayama-u.ac.jp.

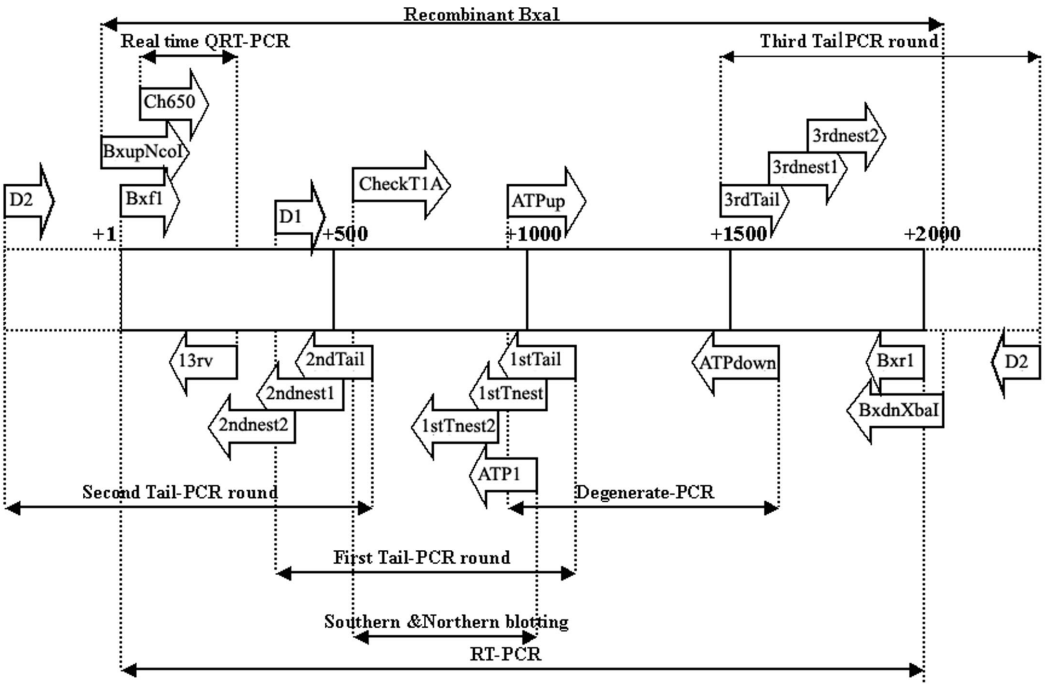

FIG. 1. Schematic diagram of the primers used in this study. Solid boxes, Bxa1 gene ORF; dotted boxes, sequences up- and downstream of the Bxa1 gene ORF; arrows, primers and their directions; dotted lines, amplified fragments and relative locations. The sequences of primers are shown in Materials and Methods.

als. This is the first CPx-ATPase that has been reported to be responsive to multiple heavy-metal ions.

MATERIALS AND METHODS

Materials and growth medium. The filamentous cyanobacterium *O. brevis* was grown at 25°C in CT medium (18, 19) modified by decreasing the concentration of Na_2-EDTA from 3 to 0.6 mg/liter. For heavy-metal induction analysis, metal salts (60 μM Zn, 16 μM Cu, 18 μM Cd, or 5 μM Ag) were added to *O. brevis* cultures grown in 2 liters of the modified CT medium for 60 days (at an optical density at 660 nm of about 0.5 in stationary phase). The cultures were then incubated for 2 h at 25°C. Cells were harvested by centrifugation at 6,000 × *g* for 5 min at 4°C, followed by three washes with Milli-Q water.

E. coli strain TOPO10 and plasmids TOPO PCR 2.1 and pBAD/Myc-His were obtained from Invitrogen (San Diego, Calif.). Terrific broth or Luria-Bertani (LB) medium (GIBCO BRL) was used for growing *E. coli*.

DNA manipulation and analysis of gene products. *O. brevis* genomic DNA was isolated by using the cetyltrimethylammonium bromide method. All DNA manipulations including digestion, purification, and plasmid extraction were performed by standard methods (28).

The PCR- or reverse transcription-PCR (RT-PCR)-amplified DNA fragment was first subcloned into the TOPO10 PCR 2.1-TOPO vectors by following the manufacturer's directions. Automated DNA sequencing was performed on an ABI 310 genetic analyzer with an ABI Bigdye terminator kit (PE Applied Biosystems). DNA sequencing results and amino acid homology and hydropathy profiles were obtained with GENETYX (Software Development Co., Ltd.).

Isolation and analysis of the putative gene encoding the P-type ATPase from *O. brevis* genomic DNA by a gradient-degenerate PCR-based method. Degenerate primers ATPup (GMRTCRTTNRYNCCRTC; sense) and ATPdown (GA YAARACNGGNACNCT; antisense) (Fig. 1) were designed by focusing on the region between the conserved phosphorylation site (DKTGTL) and the ATP-binding domain (GDGINDAP). A 40-cycle PCR was performed on an Icycler (Bio-Rad Laboratories) with a gradient annealing temperature of 40 to 60°C. The target bands were purified, subcloned, and sequenced.

Analysis of the DNA segments adjacent to the degenerate PCR product by Tail-PCR. Thermal asymmetric interlaced PCR (Tail-PCR) was performed as described by Liu and Whittier (12) but with high- and low-stringency annealing temperatures of 68 and 50°C, respectively, for the supercycle. Primers used for one round of super-PCR and two rounds of nested PCR with a melting temperature of about 70°C were designed from the DNA sequence data obtained in the preceding stage. They were as follows: 1stTail1 (GGATTGAGATTCTACCTT GGCAG; antisense specific primer for the super-PCR run of the first Tail-PCR), 1stTnest1 (CAGCCATTGCCATCAAATCAGAT; antisense specific primer for the first nested-PCR run of the first Tail-PCR), 1stTnest2 (CTCCTTTTGTCA GAGTTCCTGTT; antisense specific primer for the second nested-PCR run of the first Tail-PCR), D1 (WGTCGASWGASAWGAA; sense degenerate primer for the first Tail-PCR), 2ndTail1 (TAACCGGCGAATCAGTACCTCGA; antisense specific primer for the super-PCR run of the second Tail-PCR), 2ndnest1 (AAACCGTAGCCGTCGGCGATAT; antisense specific primer for the first nested-PCR run of the second Tail-PCR), 2ndnest2 (TCAAATCGCTCTTAG AGATCCGC; antisense specific primer for the second nested-PCR run of the second Tail-PCR), D2 (STGWAWAGTSAGCTGC; sense degenerate primer for the second Tail-PCR and antisense degenerate primer for the third Tail-PCR), 3rdTail (AAATTGGGTGTTGAGCGCATCG; sense specific primer for the super-PCR run of the third Tail-PCR), 3rdnest1 (CTGTAGCCGATAGTG TTGCGAGA; sense specific primer for the first nested-PCR run of the third Tail-PCR), and 3rdnest2 (CCGAAGGAAAAGTTGAGGCGATC; sense specific primer for the second nested-PCR run of the third Tail-PCR) (Fig. 1).

The products from the second nested PCR were separated by agarose gel electrophoresis and sequenced after being subcloned into the PCR 2.1 vector.

Southern and Northern blotting analyses. Southern and Northern blotting analyses were performed by standard methods (28). Genomic DNA (2 μg) extracted from *O. brevis* was digested with *Hin*dIII, *Eco*RII, and *Hin*cII (Toyobo). The probe used for hybridization was generated by PCR using primers CHECKT1A (CACATCTGCACTAACCGGCGAATC; sense) and ATP1 GGA TTGAGATTCTACCTTGGCAG; antisense) (Fig. 1), labeled with a PCR DIG probe synthesis kit (Roche Diagnostics GmbH).

Total RNA was isolated with the RNeasy preparation kit (Qiagen) in accordance with the manufacturer's instructions after disruption with a mortar and pestle. Contamination by DNA was eliminated by treating the total RNA with RNA-free DNase (Takara). An in vitro transcript RNA encoded by the same fragment as for Southern blotting was used as a probe, and 10 μg of total RNA was used for Northern blotting.

Analysis of heavy-metal induction by RT-PCR. A two-step RT-PCR method and a pair of primers encompassing the entire Bxa1 gene (1,983 bp), Bxf1 (ATGCAAAAAGCCAAATCGAGCGA; sense) and Bxr1 (CTTTAAAACTCT AGTTGCATTGAAAATAG; antisense) (Fig. 1), were employed in this study. The products of RT-PCR were analyzed by agarose gel electrophoresis and confirmed by automatic DNA sequencing on an ABI 310 genetic analyzer. A negative control (RT control) in which reverse transcriptase was not added to the RT-PCR solution was employed at the same time.

Quantification of transcription by real-time QRT-PCR. Real-time quantification RT-PCR (QRT-PCR) analysis was carried out with the Smart Cycle system (Cepheid) using a One Step real-time PCR kit (Qiagen). A 150-bp fragment specific for a histidine-rich motif at the N terminus of Bxa1, encompassed by primers CH650 (AGCCAAATCGAGCGATTCCG; sense) and 13rv (GGCGT GTTGTGCAGTTTTTC; antisense) (Fig. 1), was employed as the quantitative target.

The absolute amount of Bxa1 RNA in total RNA was determined by using external standards. Part of the Bxa1 gene including the target fragment was amplified by PCR, and then the amplification product was ligated into TA cloning vector pCR2.1 (Invitrogen) to create pCRSTD. This construct was used to generate standard curves in the QRT-PCR after in vitro transcription to RNA with the MEGAscript in vitro transcription kit (Ambion Inc.). The concentration of RNA was determined and used to calculate copy numbers. The kinetics curve was defined by a cycle threshold value (Ct), which marks the cycle number during the logarithmic phase at which the fluorescence of a given sample becomes significantly different from the baseline signal. Each QRT-PCR experiment was repeated three times, and the RNA extraction for each metal was performed at least twice. All experiments obtained similar results.

The validity of real-time QRT-PCR products was confirmed by melting-curve analysis from 60 to 95°C at 0.1 to 1.0°C/s. PCR products were reconfirmed by agarose gel electrophoresis (2.5%) and automatic DNA sequencing.

Construction of an *E. coli* strain with recombinant Bxa1 and analysis of heavy-metal tolerance. The cDNA of Bxa1 was generated by PCR using *O. brevis* genomic DNA as a template and oligonucleotide primers MtupNcoI (ACACC ATGGAAAAAGCCAAATCGAGCG; sense) and MtdnXbaI GCCGTCTAGA TTAAAACTCTAGTTGCA antisense) (Fig. 1). These two primers were designed to encompass the entire Bxa1 gene with the following restriction sites added: forward, *Nco*I site; reverse, *Xba*I site. The resulting 1,993-bp products were subcloned into the pBAD/Myc-His B vector to construct plasmid pBAD/Bxa1. The sequence of the recombinant gene was confirmed by automatic DNA sequencing. *E. coli* TOPO10 cells were transformed with pBAD/Bxa1 or pBAD/Myc-His B (vector control).

For the expression of Bxa1, 1 ml of Bxa1 transformant or control culture incubated overnight was inoculated into 10 ml of LB medium supplemented with 0.0002% L-arabinose and 50 μg of ampicillin/ml. The cells were then incubated at 37°C with vigorous shaking for 3 h. The transformation and expression were confirmed by PCR amplification and Western blot analysis.

Metal tolerance of the Bxa1 transformant was analyzed by inoculating 5 μl of the medium described above into 250 μl of LB medium containing 0.0002% L-arabinose, 50 μg of ampicillin/ml, and the metal ion from zinc chloride (1,000 to 2,000 μM), cadmium sulfate (500 to 1,500 μM), copper sulfate (3,000 to 5,000 μM), or silver nitrate (50 to 150 μM). The Bioscreen C microbiology analyzer (Labsystems) was employed to monitor in situ the amplification efficiency of *E. coli* strains at 30°C by measuring the absorbance at 600 nm for 24 h with intermittent agitation.

SDS-PAGE and Western blotting of the protein isolated from the recombinant *E. coli* strain. *E. coli* (2 ml) incubated overnight was inoculated into 100 ml of LB medium supplemented with ampicillin (50 μg/ml). When the optical density of the cell culture at 550 nm reached 0.5, 0.0002 or 0.02% L-arabinose was added to induce expression. Cells were collected after 4 h and washed three times with 10 mM Tris-MES (morpholineethanesulfonic acid) (pH 7.3) buffer. The pellets were then resuspended in 2 ml of the above buffer supplemented with 0.25 M sucrose, 2 mM dithiothreitol and 1 mM phenylmethylsulfonyl fluoride and disrupted by ultrasonication. The homogenate was incubated for 30 min after addition of 0.02 mg of DNase I/ml and 2 mM $MgCl_2$. Lysed cells were centrifuged at 8,000 × *g* for 20 min. The supernatant (25 μg of protein/lane) was then loaded on a sodium dodecyl sulfate–10% polyacrylamide gel electrophoresis (SDS–10% PAGE) gel for electrophoresis. A polyclonal antibody to Bxa1 was raised against a 15-mer synthesized oligopeptide (CSHDAHHEHSHENHN) designed from the histidine-rich N terminus of Bxa1 and purified after 4 months by repeated injections ($n = 8$) in rabbits.

The samples separated by SDS-PAGE were electroblotted to polyvinylidene difluoride membrane and immunodetected with the antibody described above (28).

Nucleotide sequence accession number. The nucleotide sequence data reported in this paper appear in the DDBJ, EMBL, and GenBank databases under accession no. AB073990.

RESULTS

Isolation and sequence analysis of putative CPx-ATPase by degenerate PCR and Tail-PCR. P-type ATPases contain a highly conserved phosphorylation site (DKTGTL) and ATP binding domain (GDGINDAP) (13). Computer analysis by Blast has revealed that the amino acid sequence region between these two domains is remarkably shorter in CPx-ATPase than in other P-type ATPases such as H^+-ATPase or Ca^{2+} or K^+-ATPase. These characteristics make it possible to isolate the putative CPx-ATPase directly from genomic DNA using a PCR-based method.

First, a gradient-degenerate PCR method was employed to amplify the large cytoplasmic domain between the conserved phosphorylation site and ATP binding domain by using *O. brevis* genomic DNA as a template (Fig. 1, degenerate-PCR). A 600-bp band appeared at all annealing temperatures, and its size was consistent with that for CPx-ATPase. Therefore, the 600-bp fragment was excised and subcloned into the TOPO10 vector for DNA sequencing. The sequencing data showed that the amino acid sequence encoded by this 600-bp fragment has high homology to P-type CPx-ATPase.

Tail-PCR-based methods were chosen for sequencing upstream and downstream of this fragment. Tail-PCR uses three long specific primers and one short arbitrary primer; the specific target products can usually be obtained after one round of super-PCR followed by two rounds of nested PCR. This method was successfully used to isolate the insert end segments from P1 and YAC clones (12). When it was employed to analyze the fragment from *O. brevis* genomic DNA directly, a very high background in agarose gel electrophoresis was detected, and it was impossible to identify the target products. This result may be due to the complexity of genomic DNA and the high degeneracy of the arbitrary primer. Therefore, in this study, we first designed several relatively low-degeneracy primers. Two of these primers (D1 and D2; Fig. 1) were chosen for the Tail-PCR experiment using *O. brevis* genomic DNA as a template.

The super-PCR run in the first Tail-PCR (Fig. 1, first Tail-PCR round) gave a high background pattern in agarose gel electrophoresis, and we could not separate main products in this step. However, after the second run of the nested PCR, only two specific bands at 550 and 750 bp, responding to the third specific primer, were amplified (data not shown). Each of these two bands was excised and sequenced. The DNA sequence of the 750-bp product revealed that this fragment contains a putative heavy-metal transmembrane domain, Cys-Pro-Cys, which is thought to exist only in the heavy-metal transport P-type ATPases. Further analysis revealed that the product of 550 bp belongs to the 750-bp fragment and is produced when the degenerate primers annealed to a homologous sequence which exists within the 750-bp fragment.

However, the 5′ sequences of the products of the first Tail-PCR were still incomplete, and so a second round with another degenerate primer, D2, was performed (Fig. 1, second Tail-PCR round). A 1,000-bp product (data not shown) was ob-

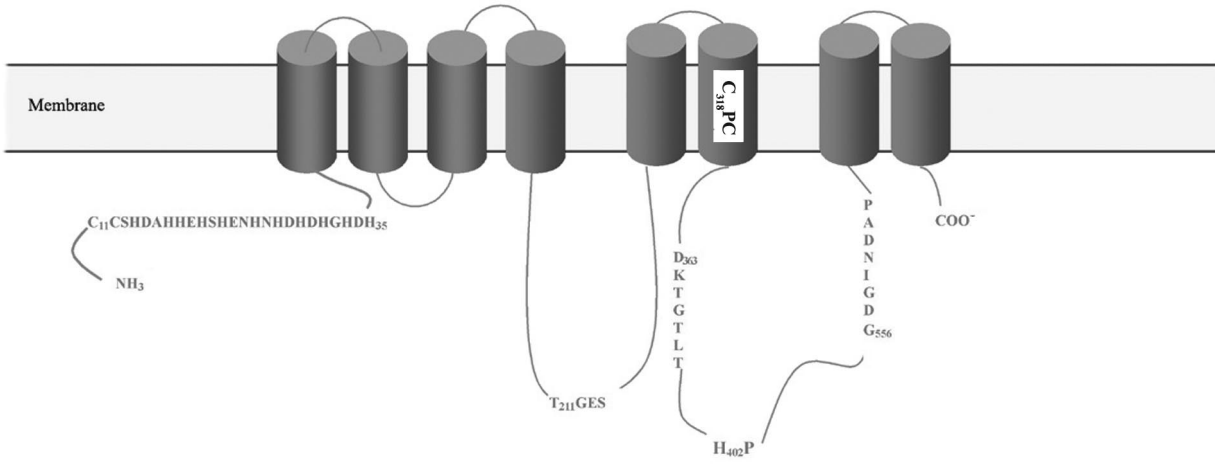

FIG. 2. Structural model of Bxa1 generated by hydropathy plot analysis. The analysis was by the method of Kyte and Doolittle using GENETYX software. Cylinders, predicted transmembrane helices. The residues conserved in CPx-ATPase are shown.

tained after the second nested PCR. Sequence analysis showed that this fragment encompassed the entire portion of the open reading frame (ORF) encoding the N terminus.

A third round of Tail-PCR was performed to identify the sequence adjacent to the 3′ sequences of the degenerate PCR products (Fig. 1, third Tail-PCR round). A fragment of about 700 bp was isolated and sequenced (data not shown).

After the third Tail-PCR, a complete 1,983-bp ORF was obtained (Fig. 1). The sequence data revealed that the gene encoded a novel putative CPx-ATPase (Bxa1).

The hydropathy analysis of the amino acid sequences predicted that Bxa1 contains eight transmembrane domains (Fig. 2). The CPC motif and HP locus are found in the sixth transmembrane domain and in the large cytoplasmic domain, respectively, which are only found in CPx-ATPase. Figure 3 shows that the N-terminal region of novel putative CPx-ATPase Bxa1 contains a unique CC sequence element and a histidine-rich motif as a putative metal binding site (see Discussion).

Genomic Southern blotting, RT-PCR, and Northern blotting. Southern blotting was performed to estimate the copy number of the Bxa1 gene in the chromosomal DNA of *O. brevis*. The same restriction patterns (one main band and one light band produced by *Hin*dIII, *Eco*RII, and *Hin*cII) were detected (Fig. 4), which suggested that the Bxa1 gene is a multiple-copy gene.

In the Northern blotting experiment, high-level transcription of the Bxa1 gene (data not shown) was observed in *O. brevis* samples incubated in medium containing Cd^{2+} or Zn^{2+}, and this transcription was much higher than in the wild-type control. This result revealed that gene expression could be enhanced by divalent heavy metals (Cd^{2+} and Zn^{2+}). Surprisingly, the transcription of the Bxa1 gene was also detected in *O. brevis* samples exposed to monovalent heavy metals (Ag^{+} and Cu^{+}) with almost the same levels of expression. RT-PCR gave a similar result (data not shown).

However, although the RT-PCR method gives a 1,000-fold-higher sensitivity than Northern blotting, it still is difficult to estimate which metal produces the higher transcription rate.

Quantitative analysis of metal-induced Bxa1 gene transcription in vivo by real-time QRT-PCR. A real-time QRT-PCR method was established to study the absolute amount of Bxa1 mRNA induced by divalent metal ions Cd^{2+} and Zn^{2+} and monovalent metal ions Ag^{+} and Cu^{+}. Real-time QRT-PCR detection methods allow the calculation of a cycle threshold (Ct) based on fluorescence. Ct values are inversely proportional to the log of the initial template mRNA concentration and are used to calculate transcript copy numbers. Before real-time QRT-PCR, the specificity of the two primers (Fig. 1, real-time QRT-PCR) was first confirmed by PCR using extracted genomic DNA from *O. brevis* as a reference (data not shown).

To generate a standard curve for absolute quantification analysis, 5- to 10-fold serial dilutions of in vitro transcription RNA from plasmid PCRSTD were employed. The calibration curve generated by the five different concentrations of RNA is

BXA1(*O. brevis*): MQKAKSSDSGCCSHDAHHEHSHENHNHDHDHGHDHGNGDFNLKQELIPVISVVLLFIGGLIFEEKLHNTPYSIAEYLVFIPAYLLSGWNVLT

CadA(*P. putida*): MNQPVSHEHKHDH.HAHSCCGSAAAPALVQLSEKA.SSHAQFSRFRIEAMDCPTEQTLIQDKLGKLAGI……

AAA62113(*E. coli* HRA1): MRNNKQHSSHSHHNHGDMEHSKHDHNEMEHSQMDHSAMGHCAMGGHAHHHHGDMDHSKHDHNEMKHSQMDHSKMDYSEMDHGAMGGHAHHHH

AAA62114(*E. coli* HRA-2): MIAYHIKKRRRHPMRDEHEHQHDHEHHQHQDHTAMSGHNMHHEHHEMAMTHDDHDASHTMRHDHAAMAHHHMHMSDDPGMAHMDMTDMGRRF

P05425(*E. hirae* CopB): MNNGIDPENETNKKGAIGKNPEEKITVEQTNTKNNLQEHGKMENMDQHHTHGHMERHQQMDHGHMSGMDHSHMDHEDMSGMNHSHMGHENMS

CAB16773(*A .thaliana*): MEPATLTRSSSLTRFPYRRGLSTLRLARVNSFSILPPKTLLRQKPLRISASLNLPPRSIRLRAVEDHHHDHHHDDEQDHHNHHHHHHQHGCC

Q59998(*Synechocystis* ZiaA): MTQSSPLKTQQMQVGGMDCTSCKLKIEGSLERLKGVA……SEITIQERIAALGYTLAEPKSSVTLNGHKHPHSHREEGHSHSHGAG

FIG. 3. Alignment of the N-terminal regions of histidine-rich putative heavy-metal transport P-type ATPases from *P. putida* (11), *E. coli* (34), *E. hirae* (30), *A. thaliana* (37), and *Synechocystis* sp. strain PCC 6803 (33). The adjacent cysteine motif and repeat HX motifs are highlighted.

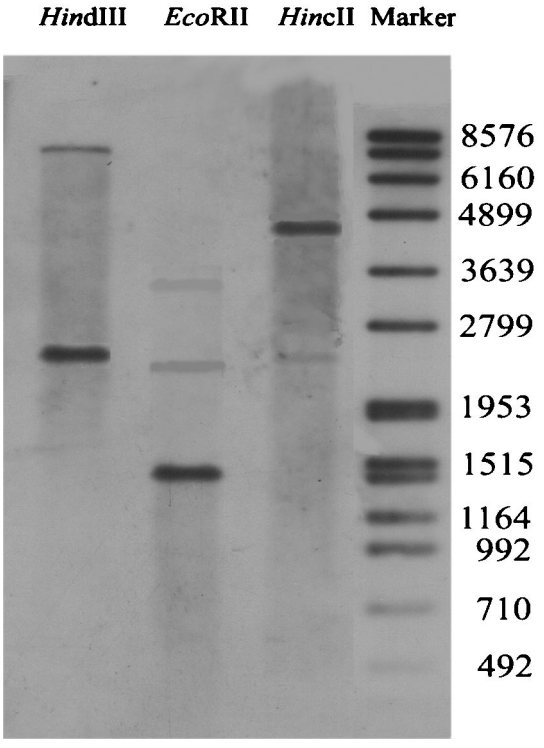

FIG. 4. Southern hybridization of Bxa1 from *O. brevis* using a digoxigenin-labeled probe. The total genomic DNA isolated from *O. brevis* was digested with *Hin*dIII, *Eco*RII, or *Hin*cII. Sizes of DNA markers are in base pairs.

shown in Fig. 5A, and a relative standard deviation of 0.9991 was obtained. For each standard RNA concentration, a single PCR product of the expected size was detected by agarose gel electrophoresis (data not shown). Amplicon fidelity was confirmed by melting-curve analysis, and the results showed that all the products have almost the same melting temperature, around 82.75°C (data not shown).

By using real-time QRT-PCR, we detected and accurately quantified the initial copy numbers of Bxa1 mRNA contained in template total RNA (Fig. 5). The highest level of transcription was determined in Zn^{2+}-supplemented samples, which contained 4.37×10^4 (Ct = 17.70) copies in 150 ng of total RNA. This result was 1.5-fold higher than that for Cd^{2+} (3.57×10^4 copies; Ct = 18.33). For the monovalent ions, 3.27×10^4 (Ct = 18.47) copies in the initial template were detected in Cu^{+}-supplemented samples, an induction similar to that for Cd^{2+}. Ag^{+} produced the lowest level of Bxa1 mRNA induction; however, it produced 2.51×10^4 copies (Ct = 18.69). In the wild-type control (without heavy metal), there were only 6.97×10^2 (Ct = 24.62) copies in the template total RNA.

For the RT control, after 30 cycles in our experimental conditions, no amplification signals were found for the specific PCR products, ensuring that the initial RNA templates were not contaminated by residual genomic DNA.

As described above, the real-time QRT-PCR results emphasized that the transcription of the Bxa1 gene can be induced by both monovalent and divalent heavy-metal ions at high levels. Zn^{2+} has more ability to induce the Bxa1 gene than other heavy-metal ions.

Expression of Bxa1 in *E. coli* strain TOPO10 confers tolerance to both monovalent and divalent heavy metals. To ensure that the polyhistidyl group at the C terminus encoded by the vector does not influence the resistance of *E. coli* to heavy metals, a stop codon was included at the end of the Bxa1 gene to remove the polyhistidyl group encoded by the vector when the Bxa1 gene was subcloned into the vector of pBAD/Myc-His B. The successful expression of Bxa1 induced by L-arabinose was confirmed by SDS-PAGE of the soluble membrane fraction isolated from *E. coli* (Fig. 6A) and Western blotting (Fig. 6B). The results showed that 0.0002% L-arabinose could induce the expression of enough Bxa1 in the membrane of *E. coli*. At a higher level of expression, Bxa1 easily forms inclusion bodies; therefore, 0.0002% L-arabinose was used for the analysis of metal sensitivity.

The growth of the *E. coli* strain TOPO10 transformed with plasmid pBAD/Bxa1 was compared to that of TOPO10 transformed with pBAD/Myc-His B (vector control) by monitoring

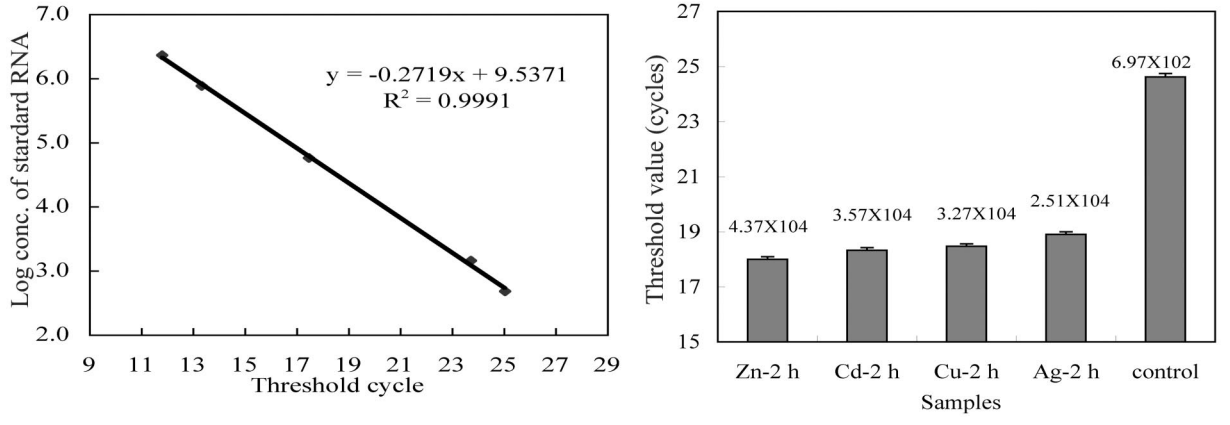

FIG. 5. Quantitative analysis of metal-induced Bxa1 gene transcription by real-time QRT-PCR. Total RNA was extracted from *O. brevis* incubated in Zn- (60 μM), Cu- (16 μM), Cd- (18 μM), and Ag (5 μM)-supplemented CT cultures or in cultures without (control) heavy-metal ions for 2 h. (A) Standard curve of Bxa1 RNA. (B) Cycle threshold and copy numbers of Bxa1 mRNA in 150 ng of total RNA determined as indicated in Materials and Methods.

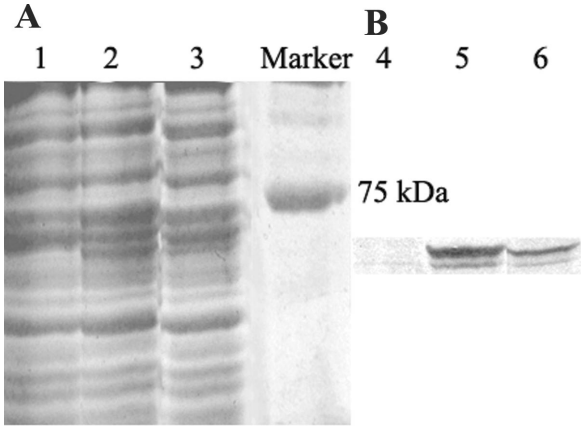

FIG. 6. Expression of Bxa1 in *E. coli* strain TOPO10. (A) SDS–10% PAGE analysis of a Coomassie blue-stained gel containing the soluble membrane fractions from *E. coli* TOPO10/pBAD/Myc-His B (vector control, lane 1), *E. coli* TOPO10/pBAD/Bxa1 treated with 0.02% L-arabinose for 4 h (lane 2), and *E. coli* TOPO10/pBAD/Bxa1 treated with 0.0002% L-arabinose for 4 h (lane 3). (B) Western blotting of the samples shown in panel A. Immunostaining was performed with an antibody raised against the synthesized peptide in the N-terminal histidine-rich region of Bxa1. Lane 4, vector control; lane 5, 0.02% L-arabinose; lane 6, 0.0002% L-arabinose.

in situ growth in LB medium supplemented with a variety of metal salts and 0.0002% L-arabinose (Fig. 7). When 1,500 μM Zn was added (Fig. 7A), the first detectable increase in the growth rate of TOPO10 carrying pBAD/Bxa1 could be observed at 3 h. For the vector control (pBAD/Myc-His B), the first detectable increase was found after 13 h, which suggested that the expression of Bxa1 conferred tolerance to zinc. Similar results were obtained when 1,000 μM Cd was added (Fig. 7B). For Cd, the first detectable increase for the pBAD/Bxa1 strain was 12 h earlier than that for the vector control strain. For the monovalent heavy metals, when the concentration of Ag was higher than 100 μM, the vector control strain stopped growing within 22 h and the growth of the Bxa1 transformant could be detected at an Ag concentration as high as 130 μM within 20 h although the first detectable increase was also delayed slightly when the concentration of Ag^+ increased (Fig. 7C). A gradual decrease in the growth rate with an increase in the heavy-metal concentration for both the Bxa1 transformant and vector control was also observed when we used other heavy-metal ions (data not shown). The same results were also obtained from Cu-supplemented media, although, due to the high concentration of copper sulfate solution, copper blue gives a very high background for spectral analysis (data not shown). As a blank control (Fig. 7D), the empty vector control strain showed higher growth saturation.

DISCUSSION

Bxa1 is a putative heavy-metal transport ATPase. In most cases, CPx-ATPases contain a highly conserved characteristic cysteine-rich $(CXXC)_n$ domain for heavy-metal binding in the polar amino-terminal region. In a few cases, it is replaced by a histidine-containing motif. Recent studies have focused on the cysteine-rich CPx-ATPase (9, 20, 23, 25, 29), with little research done on the histidine-rich CPx-ATPase.

In this study, we identified a novel gene (the Bxa1 gene) encoding a heavy-metal transport P-type ATPase with two

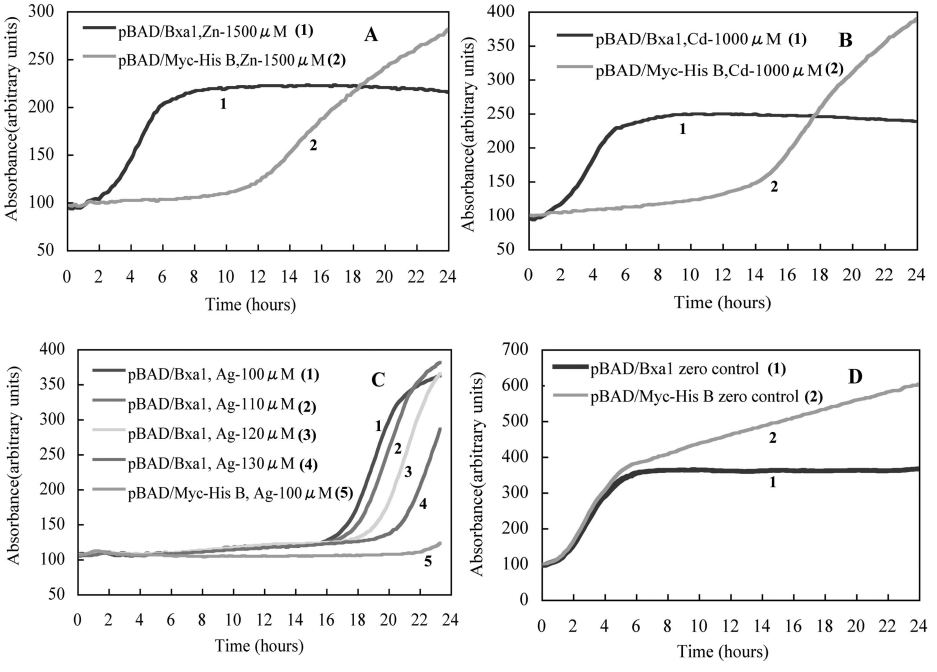

FIG. 7. In situ monitoring of the growth of *E. coli* strain TOPO10 transformed with plasmid pBAD/Bxa1 or pBAD/Myc-His B (vector control) in LB medium supplemented with a variety of metal salts and 0.0002% L-arabinose. (A) Zn; (B) Cd; (C) Ag; (D) blank control without metal ions. The growth rates of strains were monitored on line by Biosystem C at an absorbance of 600 nm for 24 h.

adjoining cysteine residues followed by a histidine-rich motif at the N terminus (11 histidines) from the filamentous cyanobacterium *O. brevis* using a PCR-based method (Fig. 2 and 3). The ORF of the Bxa1 gene encodes 660 amino acids with a predicted molecular mass of about 74 kDa (Fig. 2). A sequence homology search by Blast (http://www.blast.genome.ad.jp/) revealed that the Bxa1 gene encoded an amino acid sequence which shares high alignment scores with the heavy-metal transport P-type ATPases, especially with the divalent-heavy-metal (Zn and Cd) transport CPx-ATPase. As shown in Fig. 2, Bxa1 contained the most conserved motifs among all P-type ATPases; including a D^{363}KTGTLT motif, which is phosphorylated by ATP in the reaction cycle, a T^{211}GES motif, which functions as a phosphatase domain, and an ATP binding motif (G^{556}DGIND). Bxa1 also contains the putative heavy-metal cation transduction channel C^{318}PC and conserved H^{402}P dipeptide. The last two motifs have not been found in other P-type ATPases except for CPx-ATPases. Hydropathy plot analysis showed that Bxa1 traverses the membrane eight times, like other CPx-ATPases found in humans and bacteria (2, 15, 25, 31) but unlike the non-heavy-metal P-type ATPases, which usually possess 10 or more transmembrane regions (13, 37). The CPC motif was found in the sixth transmembrane helix, whereas for the non-heavy-metal P-type ATPases such as Ca^{2+}-ATPases or H^+-ATPases a similar motif is located in the fourth transmembrane region. H^{402}P is in the large cytoplasmic domain, as expected in Bxa1. This motif corresponds to the conserved HP locus, which is only found in CPx-ATPase.

Bxa1 also contained an N terminus cytoplasmic domain (Fig. 3) which is thought to be involved in metal binding, though it is quite different from that in other CPx-ATPases. First, the N terminus cytoplasmic domain of Bxa1 (42 amino acids) was shorter than those of common CPx-ATPases (more than 100 amino acids). Second, two adjoining cysteine residues followed closely by high-density histidine repeats were identified instead of the common heavy-metal binding domain (CXXC or relatively low-density histidine motifs). The two adjoining cysteines (C^{11}C) are uncommon in CPx-ATPase and have only been found in the prolonged carboxyl termini of unidentified putative Zn/Co/Cd/Pb ATPases HMA2 and HMA4 from *Arabidopsis thaliana* (10, 13), and it has been proposed that this domain is involved in heavy-metal binding. Similar CC motifs also exist in plant Zn and Cu metallothioneins (27), a group of cysteine-rich proteins that sequester heavy metals, and function as part of the heavy-metal binding motif (20). A histidine-rich motif in the N-terminus also occurs in certain CPx-ATPases (Fig. 3) (11, 33, 34, 37). In these CPx-ATPases, a histidine-rich motif was thought to be a putative heavy-metal binding domain, although in most cases the histidine content and density were not as high as in those for Bxa1. The histidine-rich domain, especially the repeat of HX at the N terminus, is usually associated with divalent ions such as Zn^{2+}, Cd^{2+}, Co^{2+}, Pb^{2+}, and Ni^{2+}, although histidine-rich CPx-ATPase CopB (21) was found to transport only monovalent metals, such as Cu^+ and Ag^+. In Bxa1, the Cys-Cys motif following the histidine-rich domain should be included in the heavy metal binding site.

Bxa1 confers tolerance to both monovalent and divalent heavy metals. CPx-ATPases have been thought to display a high specificity for the heavy metals to be transported. They can be further subdivided into two classes: those that transport monovalent heavy metals such as Cu^+ and Ag^+ (2, 16, 20, 26, 32, 39) and those that transport divalent soft metals such as Zn^{2+} and Cd^{2+} (1, 25, 29, 31, 37).

In this study, the transcription of Bxa1 mRNA increased remarkably when heavy metals were present in the growth medium. Northern blotting and RT-PCR revealed that Bxa1 is responsible for transporting not only divalent metals (Zn^{2+} and Cd^{2+}) but also monovalent metals (Ag^+ and Cu^+). This behavior was quite different from that of CPx-ATPases known so far. However, it is impossible to distinguish the induction properties among these metals by Northern blotting and RT-PCR. Therefore, a real-time QRT-PCR method was employed to study the in vivo induction for a variety of metals. This method allows the quantitative measurement of mRNA levels in small quantities with high sensitivity and accuracy.

The copy number of Bxa1 mRNA in Zn^{2+}-supplemented samples is 63-fold higher than that of the wild-type control (without heavy metal) (Fig. 5). The number of copies of Bxa1 mRNA induced by Cd^{2+} was one-fifth of that induced by Zn^{2+}, indicating that both Zn^{2+} and Cd^{2+} might be substrates for Bxa1. However, the expression of Bxa1 mRNA was also highly induced by Cu^+: the 3.27×10^4 copies of Bxa1 mRNA induced by Cu^+ were almost the same number induced by Cd^{2+}. Another monovalent heavy metal, Ag^+, induced about 80% of the Bxa1 mRNA induced by Cd^{2+} and Cu^+. In terms of the transcription ability of Bxa1, the heavy metals ranked as follows: $Zn^{2+} \geqq Cd^{2+} = Cu^+ \geqq Ag^+$. Zn^{2+} is the most efficient inducer of Bxa1 mRNA, revealing that the primary function of Bxa1 may be related to zinc metabolism. However, if we hypothesize that Bxa1 is a Zn^{2+} transporter, the dominance of Zn^{2+} is poor compared with that for other CPx-ATPases because the difference between Zn^{2+} and Ag^+ is only 40%. The mRNA expression of ziaA (divalent cation translocating CPx-ATPase from *Synechocystis* sp. strain PCC 6803) is induced only by Zn^{2+} and cannot be induced by Cu^+ and Ag^+ (33). On the other hand, the expression of mRNA of CRD1 (a monovalent cation transport CPx-ATPase from *Candida albicans*) increased approximately 14- and 32-fold on exposure to 0.1 and 1 mM $CuSO_4$, respectively, and exposure of cells to 0.1 and 1 mM $CdSO_4$ led to only a 2- to 3-fold induction (23). Based on the studies described above, Bxa1 gene transcription can be highly induced by both monovalent and divalent cations.

In the time course analysis of the growth rates of *E. coli* TOPO10 strains, the Bxa1 transformants showed higher rates of growth than the vector control strains at toxic levels of Zn, Cd, Cu, or Ag salt. These results indicated that Bxa1 mediates tolerance to both divalent and monovalent heavy metals. This tolerance in vitro is consistent with the results of in vivo real-time QRT-PCR (Fig. 5). All reports to date show that the CPx-ATPases have high specificity for the ion valence or variety of the heavy metal to be transported; CRD1 was found to confer a high level of resistance to Cu^+ and Ag^+ but little resistance to Cd^{2+} and none to Zn^{2+} (23). On the other hand, the sensitivity of the ziaA disruption mutant to Cd^{2+} and Zn^{2+} increased markedly compared with the that for the wild strain, but no difference was observed for Cu^+ and Ag^+ (33). Based on our study described above, it can be concluded that the Bxa1 gene is responsible for both monovalent and divalent

cations and mediates both monovalent and divalent heavy-metal cation cotolerance.

Our knowledge of the heavy-metal specificity of CPx-ATPases is poor, although there has been much effort to understand the role of the heavy-metal binding domains in metal specificity. One hypothesis about the existence of a recognition site was made (37). Those analyses of the amino acid sequence of the N-terminal cysteine-rich CPx-ATPase suggested that a leucine residue (the 21st residue downstream from the last CXXC) might be involved in conferring Cu^+ specificity on the metal binding domain, and tyrosine or phenylalanine instead of leucine at this position responds to Zn^{2+} and Cd^{2+} (37). However, we did not find the signal amino acid residues predicted above (the 21st downstream from CC). No effort to study metal ion recognition and specificity in histidine-rich CPx-ATPases has been made, because only a few of them have been identified so far. In most cases, histidine-rich CPx-ATPases tend to mediate divalent-heavy-metal transduction, especially for Zn^{2+}. Relatively histidine-poor CPx-ATPases such as the CopB series from *Enterococcus hirae* (30) function as Cu^+ and Ag^+ transporters. How the histidine-rich CPx-ATPases achieve specificity for the substrate to be transported is still unknown. Another mechanism should be involved in the heavy-metal specificity of Bxa1.

It has been also suggested that the specificity of the metal binding domain leads to the specificity of CPx-ATPase metal transport (1, 6, 7, 9). In an immobilized-metal affinity chromatographic study, we found that recombinant Bxa1 has the ability to bind both monovalent and divalent heavy-metal ions (unpublished data). However, recent studies on metal binding domains of Menkes and Wilson CPx-ATPases illustrated that they can also bind both monovalent and divalent heavy metals but that the divalent heavy metals are not the substrates for its function (4, 14). Some of the CPx-ATPases found in other organisms to date also show the ability to bind multiple heavy metals but display a high-stringency specificity for the heavy-metal ions to be transported (7, 36). These studies suggest that heavy-metal binding to the N-terminal binding domain might not mean the transportation of this metal.

Bxa1 has a high level of homology with the other CPx-ATPases as we described above, especially to the sequence of the downstream N-terminal cytoplasmic domain. Blast homology analysis showed that the amino acid sequence downstream of the first predicted transmembrane domain in Bxa1 has 71% identity with ziaA but only 2% identity at the N terminus. Bxa1 contains a pair of adjoining cysteine residues and a rich $(HX)_n$ repeat domain, which was speculated to function as a putative metal binding site (Fig. 2). A similar Cys-Cys pair was found in a putative cadmium transport CPx-ATPase from *Pseudomonas putida* (AF333916) and a recently identified Zn^{2+}-specific transport CPx-ATPase from *A. thaliana* (CAB16773) (Fig. 3), both of which also contained a histidine-rich domain but did not show a multi-heavy-metal response. It is noted that ziaA also contains an $(HX)_4$ motif at the 63rd residue downstream of cysteine; however, ziaA proved to be specific for only divalent heavy metals. As shown in Fig. 3, the density, arrangement, and locus of histidines in the Bxa1 N terminus was quite different from those of the other N-terminal histidine-rich ATPases. Although the real role of the heavy-metal binding domains in the function and transport specificity of CPx-ATPase remains to be found, the low specificity of Bxa1 for the substrates to be transported should be related not only to the unique heavy-metal binding domain but also to the unique amino acid sequence in the N-terminal cytoplasmic domain. A study of the function of the two adjoining Cys residues and histidine-rich motif in Bxa1 may help us to understand the role of the N-terminal heavy-metal binding domain in the function of heavy-metal transport ATPases.

In conclusion, we identified a novel CPx-ATPase with a histidine-rich N terminus from the filamentous cyanobacterium *O. brevis*. The evidence presented in this paper demonstrates that Bxa1 is induced by both divalent and monovalent heavy metals at almost the same level and conferred resistance to multiple heavy-metal ions. This is the first report of a CPx-ATPase responsive to both monovalent and divalent heavy-metal ions.

ACKNOWLEDGMENTS

This work was partially supported by grants from the Sumitomo Foundation (to S.N.) and from the Oohara Foundation for Agricultural Sciences and Grants-in-Aid for Scientific Research from the Ministry of Education, Culture, Sports, Science and Technology of Japan. (no. 11440237 to K.K.; no. 10878087 to S.N.)

We thank the Norwegian Institute for Water Research for providing *O. brevis*.

REFERENCES

1. **Binet, M. R., and R. K. Poole.** 2000. Cd^{2+}, Pb^{2+} and Zn^{2+} ions regulate expression of the metal-transporting P-type ATPase ZntA in *Escherichia coli*. FEBS Lett. **473:**67–70.
2. **Bull, P. C., and D. W. Cox.** 1994. Wilson disease and Menkes disease: new handles on heavy-metal transport. Trends Genet. **10:**246–252.
3. **Clemens, S.** 2001. Molecular mechanisms of plant metal tolerance and homeostasis. Planta **212:**475–486.
4. **DiDonato, M., H. F. Hsu, S. Narindrasorasak, L. Que, Jr., and B. Sarkar.** 2000. Copper-induced conformational changes in the N-terminal domain of the Wilson disease copper-transporting ATPase. Biochemistry **39:**1890–1896.
5. **Eng, B. H., M. L. Guerinot, D. Eide, and M. H. Saier.** 1998. Sequence analyses and phylogenetic characterization of the ZIP family of metal ion transport proteins. J. Membr. Biol. **166:**1–7.
6. **Fan, B., G. Grass, C. Rensing, and B. P. Rosen.** 2001. *Escherichia coli* CopA N-terminal Cys(X)(2)Cys motifs are not required for copper resistance or transport. Biochem. Biophys. Res. Commun. **286:**414–418.
7. **Ferenci, P.** 1999. Ital. J. Gastroenterol. Hepatol. **31:**416–425.
8. **Herrmann, L., D. Schwan, R. Garner, H. L. Mobley, R. Haas, K. P. Schafer, and K. Melchers.** 1999. *Helicobacter pylori* cadA encodes an essential Cd(II)-Zn(II)-Co(II) resistance factor influencing urease activity. Mol. Microbiol. **33:**524–536.
9. **Jensen, P. Y., N. Bonander, N. Horn, Z. Tumer, and O. Farver.** 1999. Expression, purification and copper-binding studies of the first metal-binding domain of Menkes protein. Eur. J. Biochem. **264:**890–896.
10. **Kristian, B. A., and G. P. Michael.** 2001. Inventory of the superfamily of P-type ion pumps in *arabidopsis*. Plant Physiol. **126:**696–706.
11. **Lee, S. W., E. Glickmann, and D. A. Cooksey.** 2001. Chromosomal locus for cadmium resistance in *Pseudomonas putida* consisting of cadmium-transporting ATPase and a MerR family response regulator. Appl. Environ. Microbiol. **67:**1437–1444.
12. **Liu, Y. G., and R. F. Whittier.** 1995. Thermal asymmetric interlaced PCR: automatable amplification and sequencing of insert end fragments from P1 and YAC clones for chromosome walking. Genomics **25:**674–681.
13. **Lutsenko, S., and J. H. Kaplan.** 1995. Organization of P-type ATPases: significance of structural diversity. Biochemistry **34:**15607–15613.
14. **Lutsenko, S., K. Petrukhin, M. J. Cooper, C. T. Gilliam, and J. H. Kaplan.** 1997. N-terminal domains of human copper-transporting adenosine triphosphatases (the Wilson's and Menkes disease proteins) bind copper selectively in vivo and in vitro with stoichiometry of one copper per metal-binding repeat. J. Biol. Chem. **272:**18939–18944.
15. **Melchers, K., T. Weitzenegger, A. Buhmann, W. Steinhilber, G. Sachs, and K. P. Schafer.** 1996. Cloning and membrane topology of a P-type ATPase from *Helicobacter pylori*. J. Biol. Chem. **271:**446–457.
16. **Michael, J., M. J. LaGier, G. Zhu, and J. S. Keithly.** 2001. Characterization of a heavy metal ATPase from the apicomplexan *Cryptosporidium parvum*. Gene **266:**25–34.

17. **Mitra, B., and R. Sharma.** 2001. The cysteine-rich amino-terminal domain of ZntA, a Pb(II)/Zn(II)/Cd(II)-translocating ATPase from *Escherichia coli*, is not essential for its function. Biochemistry **40:**7694–7699.
18. **Naes, H., H. Aarnes, H. C. Utkilen, S. Nilsen, and O. M. Skulberg.** 1985. Effect of photon fluence rate and specific growth rate on geosmin production of the cynobacterium *Oscillatoria brevis* (Kütz.) Gom. Appl. Environ. Microbiol. **49:**1538–1540.
19. **Nakashima, S., and M. Yagi.** 1992. Iron forms that influence the growth and musty odor production of selected cyanobacteria. Water Sci. Technol. **25:** 207–216.
20. **Nourizadeh, S., J. M. Alonso, W. P. Dailey, A. Dancis, and J. R. Ecker.** 1999. RESPONSIVE-TO-ANTAGONIST1, a Menkes/Wilson disease-related copper transporter, is required for ethylene signaling in *Arabidopsis*. Cell **97:**383–393.
21. **Odermatt, A., R. Krapf, and M. Solioz.** 1994. Induction of the putative copper ATPases, CopA and CopB, of *Enterococcus hirae* by Ag^{+} and Cu^{2+}, and Ag^{+} extrusion by CopB. Biochem. Biophys. Res. Commun. **202:**44–48.
22. **Paulsen, I. T., and M. H. Saier.** 1997. A novel family of ubiquitous heavy metal ion transport proteins. J. Membr. Biol. **156:**99–103.
23. **Perry, J. R., and C. A. Kumamoto.** 2000. Role of a *Candida albicans* P1-type ATPase in resistance to copper and silver ion toxicity. J. Bacteriol. **182:**4899–4905.
24. **Rad, M. R., L. Kirchrath, and C. P. Hollenberg.** 1994. A putative P-type Cu(2+)-transporting ATPase gene on chromosome II of *Saccharomyces cerevisiae*. Yeast **10:**1217–1225.
25. **Rensing, C., M. Ghosh, and B. P. Rosen.** 1999. Families of soft-metal-ion transporting ATPases. J. Bacteriol. **181:**5891–5897.
26. **Rensing, C., B. Fan, R. Sharma, B. Mitra, and B. P. Rosen.** 2000. CopA: an *Escherichia coli* Cu(I)-translocating P-type ATPase. Proc. Natl. Acad. Sci. USA **97:**652–656.
27. **Robinson, N. J., A. M. Tommey, C. Kuske, and P. J. Jackson.** 1993. Plant metallothioneins. Biochem. J. **295:**1–10.
28. **Sambrook, J., E. F. Fritsch, and T. Maniatis.** 1989. Molecular cloning: a laboratory manual, 2nd ed. Cold Spring Harbor Laboratory, Cold Spring Harbor, N.Y.
29. **Sharma, R., C. Rensing, B. P. Rosen, and B. Mitra.** 2000. The ATP hydrolytic activity of purified ZntA, a Pb(II)/Cd(II)/Zn(II)-translocating ATPase from *Escherichia coli*. J. Biol. Chem. **275:**3873–3878.
30. **Solioz, M., and A. Odermatt.** 1995. Copper and silver transport by CopB ATPase in membrane vesicles of *Enterococcus hirae*. J. Biol. Chem. **270:** 9217–9221.
31. **Solioz, M., and C. Vulpe.** 1996. CPx-type ATPases: a class of P-type ATPases that pump heavy metals. Trends Biochem. Sci. **21:**237–241.
32. **Tabata, K., S. Kashiwagi, H. Mori, C. Ueguchi, and T. Mizuno.** 1997. Cloning of a cDNA encoding a putative metal-transporting P-type ATPase from *Arabidopsis thaliana*. Biochim. Biophys. Acta **1326:**1–6.
33. **Thelwell, C., N. J. Robinson, and J. S. Turner-Cavet.** 1998. An SmtB-like repressor from *Synechocystis* PCC 6803 regulates a zinc exporter. Proc. Natl. Acad. Sci. USA **95:**10728–10733.
34. **Trenor, C., III, W. Lin, and N. C. Andrews.** 1994. Novel bacterial P-type ATPases with histidine-rich heavy-metal-associated sequences. Biochem. Biophys. Res. Commun. **205:**1644–1650.
35. **Tsai, K. J., K. P. Yoon, and A. R. Lynn.** 1992. ATP-dependent cadmium transport by the cadA cadmium resistance determinant in everted membrane vesicles of *Bacillus subtilis*. J. Bacteriol. **174:**116–121.
36. **Voskoboinik, I., D. Strausak, M. Greenough, H. Brooks, M. Petris, S. Smith, J. F. Mercer, and J. Camakaris.** 1999. Functional analysis of the N-terminal CXXC metal-binding motifs in the human Menkes copper-transporting P-type ATPase expressed in cultured mammalian cells. J. Biol. Chem. **274:** 22008–22012.
37. **Williams, L. E., J. K. Pittman, and J. L. Hall.** 2000. Emerging mechanisms for heavy metal transport in plants. Biochim. Biophys. Acta **1465:**104–126.
38. **Woeste, K. E., and J. J. Kieber.** 2000. A strong loss-of-function mutation in RAN1 results in constitutive activation of the ethylene response pathway as well as a rosette-lethal phenotype. Plant Cell **12:**443–455.
39. **Ziva, W., B. Israela, C. Ben-Zion, and K. Daniel.** 2000. The high copper tolerance of *Candida albicans* is mediated by a P-type ATPase. Proc. Natl. Acad. Sci. USA **97:**3520–3525.